JCTC Journal of Chemical Theory and Computation

Article

pubs.acs.org/JCTC

Electronic Energy Gaps for π-Conjugated Oligomers and Polymers Calculated with Density Functional Theory

Haitao Sun[†,‡] and Jochen Autschbach*[,†]

[†]Department of Chemistry, University at Buffalo, State University of New York, Buffalo, New York 14260-3000, United States

[‡]Shanghai Key Laboratory of Advanced Polymeric Materials, Key Laboratory for Ultrafine Materials of Ministry of Education, School of Materials Science and Engineering, East China University of Science and Technology, Shanghai 200237, P. R. China

Supporting Information

ABSTRACT: In varying contexts, the terms "energy gap" (energy difference) or "band gap" may refer to different experimentally observable quantities or to calculated values that may or may not represent observable quantities. This work discusses various issues related to calculations of electronic energy gaps for organic π-conjugated oligomers and linear polymers by density functional theory (DFT). Numerical examples are provided, juxtaposing systematic versus fortuitous agreement of orbital energy gaps with observable fundamental (ionization vs electron attachment) or optical (electronic excitation) energy gaps. Successful applications of DFT using nonempirically tuned hybrid density functionals with range-separated exchange (RSE) for calculations of optical gaps, fundamental gaps, and electron attachment/detachment energies are demonstrated. The extent of "charge-transfer like" character in the longest-wavelength singlet electronic excitations is investigated.

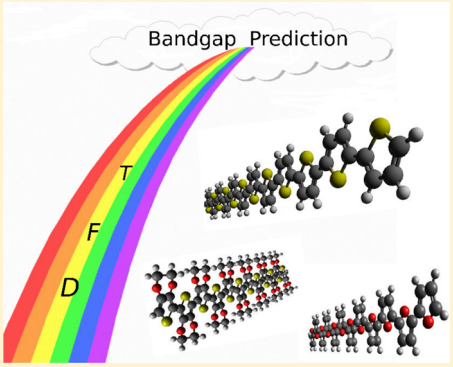

1. INTRODUCTION

"Band gaps" (vide infra) are parameters of central importance when determining possible applications of conducting polymers.[1−4] Control of band gaps is essential to enhance electroluminescence of organic light-emitting diodes (OLEDs)[5] or to improve the efficiency of light absorption in photovoltaic cells.[4,6] A search for materials with small band gaps has been motivated, for example, by the need to develop organic polymers with good nonlinear optical response[6,7] or semiconductors with high electrical conductivity.[8,9] Figure S1 in the Supporting Information (SI) documents the dramatically expanding role of quantum calculations in studies of polymer materials—in particular with Kohn−Sham (KS) density functional theory (DFT). In the process of developing novel polymer materials there is a great need to establish reliable, instructive, and computationally efficient theoretical tools to predict electronic and optical properties of π-conjugated polymers.[6]

The term band gap may have different meanings. "Band" customarily refers to the electronic structure of infinite periodic systems. In this study, we also investigate finite-size systems such as monomers of π-conjugated polymers and oligomers of different sizes. The term band gap is used here also to represent a property of the finite system that converges to the infinite-periodic (band-structure) limit as the oligomer size increases. The word "gap" indicates a difference between electronic energy levels. These can either be observable energy gaps ΔE that were measured or calculated from first principles, or some type of calculated molecular orbital (MO) or crystal orbital (CO) energy gap $\Delta\varepsilon$ such as the energy difference between the highest occupied molecular orbital (HOMO) and the lowest unoccupied one (LUMO). As an example for an observable energy gap, there is the lowest-energy optically allowed electronic excitation energy ΔE_O, which can be referred to as an (adiabatic or vertical) optical gap. Another type of energy gap is that for (adiabatic or vertical) electron attachment or electron detachment, with the associated energies being the electron affinity (EA) and the ionization potential (IP), respectively. The difference, ΔE_F = IP − EA, is the fundamental gap. Orbital energies and corresponding $\Delta\varepsilon$ such as KS DFT or Hartree−Fock (HF) eigenvalues may or may not correspond to an observable quantity. Even if a formally exact relationship exists (see below), approximations in practical calculations can lead to large errors. Moreover, it is clear that an orbital energy gap $\Delta\varepsilon$ generally cannot represent ΔE_O and ΔE_F simultaneously. In DFT calculations, interpreting the orbital energy gap as the fundamental gap is correct in principle, but with common approximations used in the functionals this interpretation is often not useful in practice.

For predicting various types of band gaps of infinite-chain conjugated polymers, a common strategy relies on extrapolation from a series of oligomers with increasing numbers, m, of monomers.[10−14] Band gaps often exhibit a roughly linear dependence on $1/m$, allowing extrapolation to $m \to \infty$, $1/m \to 0$. Generally, the quality of calculated results for different properties strongly rely on the physical models employed.[15] For extrapolations it has been pointed out that care must be taken

Received: November 19, 2013
Published: February 11, 2014

   dx.doi.org/10.1021/ct4009975 | J. Chem. Theory Comput. 2014, 10, 1035−1047

such that the infinite-periodic limit is reliably predicted from a series of oligomer calculations. Band gaps may deviate from linearity in $1/m$, requiring large m and appropriate fitting schemes.[6,16] By using periodic boundary conditions (PBCs), one can also calculate band gaps for infinite-chain length polymers directly.[16−18] A significant advantage of PBCs is that they avoid multiple calculations and extrapolation. A drawback is a typically more limited functionality of PBC quantum chemistry programs compared to their molecular counterparts.

A large number of conjugated oligomers have been studied by theoretical calculations. Semiempirical methods, such as INDO-SCI[19] and ZINDO/CIS[20] can be easily applied to large systems but they may produce unreliable band gaps for systems that are very different from those used for their parametrization. Ab-initio correlated wave function-theory methods (WFT), such as CC2,[21] CASPT2,[22,23] and CCSD-EOM[24,25] were shown to produce suitably accurate optical gaps with respect to experimental measurements, but their computational expense limits on the size of systems that can be explored. Many-body perturbation theory, such as the GW approach[26−29] popular in condensed-matter theory, is theoretically well-grounded and performs reasonably well for the prediction of band gaps. However, for many application scenarios the computational cost associated with GW may be too high.[30]

It is well-known that density functional theory (DFT) and time-dependent DFT (TDDFT) carry a computational cost that allows for a treatment of quite large systems. However, for molecules the most frequently applied functionals, viz. generalized gradient approximations (GGA) and global hybrid GGA functionals with a fixed amount of nonlocal one-determinant exact exchange (eX), afford an incorrect asymptotic behavior of the potential, significant delocalization errors, and lack of the derivative discontinuity,[31,32] which adversely impacts predictions of band gaps, in particular for long-chain conjugated systems. For instance, Louie and collaborators demonstrated there is a large variability in band gaps (ΔE_O and $\Delta\varepsilon$) calculated from different hybrid functionals, from which it was inferred that existing hybrid functionals do not produce reliable band gaps.[33] It has also been shown that nonhybrid ("pure") density functionals do not give a good correlation of the predicted orbital energy gap $\Delta\varepsilon$ with experimental absorption energies ΔE_O.[14] Savoie et al. showed that calculated orbital energies based on conventional hybrid and meta-hybrid functionals are not suitable for a predictive description of the performance of organic photovoltaics.[34] Other studies of orbital energy gaps $\Delta\varepsilon$ of conjugated oligomers and polymers using hybrid functionals found surprisingly good agreement with measured optical gaps ΔE_O.[12,16,35] However, many of the available studies confirm that the predictive power of DFT and TDDFT in this important area leaves a lot to be desired.[33,36] Inclusion of eX via hybrid functionals has been shown to ameliorate some of the problems of DFT with extended π systems.[12,37] However, calculated transfer integrals in organic semiconductors were found to be sensitive to the fraction of eX.[38]

Hybrid functionals with range-separated exchange (RSE)[32,39−43] switching from DFT to HF at increasing interelectronic distances are becoming increasingly popular in computational chemistry, for instance in the form of long-range corrected hybrids.[43,44] RSE hybrids represent a particular form of generalized Kohn−Sham (GKS)[45,46] and may significantly improve the prediction of properties of π-conjugated oligomers.[47−50] The range-separation parameter can be considered as a functional of the density.[46,51,52] An optimal range-separation parameter γ in RSE functionals may depend on the property of interest and the criteria used to decide what "optimal" means. Baer, Kronik, (BK), and collaborators have considered a nonempirical, albeit system-specific, "optimal tuning" to determine γ for RSE functionals;[46,53,54] the procedure is described in section 2.3. The range-separation parameters for RSE functionals tuned in this sense tend to be strongly system-dependent. RSE tuning significantly improves charge-transfer (CT) excitation energies which have posed a long-standing problem for TDDFT. Our group has recently applied the optimal tuning approach to a range of calculated molecular ground state and response properties and often found significant improvements over standard functionals,[48,55−58] usually because of a smaller DFT delocalization error (DE)[59] afforded by the tuned functionals. Tuning has also been shown to predict fundamental and excitation gaps in DNA and RNA nucleobases accurately,[60] it has allowed for reasonable simulations of the lowest excited states and optical absorption spectra of donor−acceptor copolymers for organic photovoltaics[61] and was even deemed "unavoidable" in studies of π-conjugated materials,[62] although not without dissent.[63] In ref 64 we further suggested a nonempirical "curvature minimization" in the tuning procedure designed to render the DE as small as possible for a given approximate functional while retaining the improvements from tuning (see section 2.3). It was subsequently shown for a set of polyaromatic hydrocarbons that optimal tuning with curvature minimization produces orbital energies that are in very good agreement with the GW quasi-particle energies used to match experimental photoelectron spectra.[65]

With an optimally tuned RSE functional the orbital gap is by construction equal, or optimally close, to the fundamental gap ΔE_F calculated at the same level of theory. The orbital energies and their difference can then be compared directly with experiment. The optical gap ΔE_O typically is much smaller (for insulators) and can be calculated by other means such as TDDFT linear response theory. With other types of approximate functionals, the orbital energy gap $\Delta\varepsilon$ is generally numerically neither close to ΔE_O nor to ΔE_F. In the TDDFT linear response formalism, $\Delta\varepsilon$ is an approximation for an excitation energy[66] and may be numerically close to ΔE_O, depending on the system and the functional. For extended systems and approximate semilocal (nonhybrid approximate) functionals, the lowest TDDFT excitation energy numerically approaches $\Delta\varepsilon$[17,29,67] which, however, in this case also tends to underestimate significantly the correct optical gap.[17,29,67] Hybrid functionals perform better in TDDFT calculations for extended systems[68] but not necessarily with a close correspondence between $\Delta\varepsilon$ and ΔE_O. It is important in this context to mention the screened hybrid functional by Heyd−Scuseria−Ernzerhof (HSE),[69,70] which has become popular for calculations of extended periodic systems. Here, the functional has a HF exchange component at short interelectronic distances which is screened at long-range. It has been demonstrated for several insulators that the HSE orbital energy gap is close to ΔE_O as obtained from TDDFT with a corresponding nonscreened hybrid functional.[68]

In this work, we investigate different types of calculated energy gaps and their relation to experimentally observable properties, along with the performance of optimally tuned RSE functionals. If not specified otherwise, the present work considers vertical energy gaps, excluding the effects from

structure relaxation and zero-point vibration. One of the aims of this study is to show for selected conjugated oligomers and polymers under which conditions calculated orbital energies and orbital energy gaps correspond to the aforementioned observable quantities and re-examine cases where an agreement is fortuitous. Further, the delocalization error for Hartree−Fock theory and various functionals is numerically quantified for several representative systems, and for oligomers of different lengths the extent of charge-transfer in the electronic excitations is investigated. Results for oligomers with large m are compared with PBC calculations for infinite-periodic polymers. The systems that were studied are shown in Figure 1. Polythiophene (PT) is an important benchmark system.

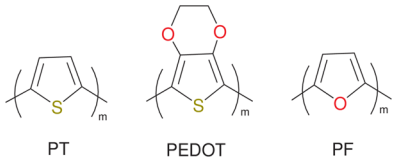

Figure 1. Systems considered in this work: polythiophene (PT), poly-3,4-ethylenedioxythiophene (poly-EDOT or PE) and polyfuran (PF), along with finite oligomers (OT, OE, OF).

Poly-3,4-ethylenedioxythiophene (PE) and polyfuran (PF) were also investigated to demonstrate the applicability of the tuning approach for related polymer systems. It is shown that optimally tuned RSE functionals perform very well for predictions of band gaps. The good performance for optical gaps, compared to the global hybrid functional B3LYP and a nonhybrid functional, appears to be related to a not insignificant CT-like character of the excitations. B3LYP gives fortuitously good agreement of orbital energy gaps with experimental optical gaps for some oligomers. The HSE functional is also investigated. We reiterate the differences between different types of energy gaps with the help of numerical comparisons from first-principles calculations.

2. COMPUTATIONAL DETAILS

2.1. General Aspects. Computations were performed with DFT and with Hartree−Fock (HF) theory, using Gaussian-type basis sets. Some of the basis sets were obtained from the Basis Set Exchange.[71] Initial ground-state geometries of all-trans α-oligomers were taken from ref 16 and reoptimized with Gaussian 2009 (G09[72]) using the hybrid functional B3LYP[73,74] and the 6-31G(d) basis set. The geometries of OT and OF were constrained to C_{2h} and C_{2v} symmetries for even and odd oligomers, respectively. OE was optimized without symmetry constraints. PBC calculations for polymers were also performed with G09, using default settings for the reciprocal space grid and other technical aspects. Other calculations were carried out with a 2013 developer's version of the NWChem 6.3 quantum chemistry package[75] incorporating functionality to perform DFT calculations with fractional electron numbers.[55,64] For the HSE functional, the HSE06 parametrization as provided in the NWChem manual was used. Iso-surface graphics of molecular orbitals (MOs) were created with the graphical user interface of the Amsterdam Density Functional package.[76]

2.2. Comparison between Calculated and Experimental Data. The main focus of this work is on the differences between various types of *calculated* energy gaps, and their correspondence to orbital energy gaps and TDDFT data. Experimental data are used for semiquantitative comparisons and guidance. Accurate predictions of experimental data by calculations are possible, of course. But the task can become rather involved, for instance due to conformational effects,[6] condensed-matter effects (solution and solid state),[6,20] differences between vertical and adiabatic energies and zero-point energy corrections,[77] and onset vs peak values in the experimental data.[77,78] For instance, the wavelength of strongest absorption intensity λ_{max} may not coincide with a calculated vertical excitation. It has been stated that the best way to determine the π-to-π^* transition energies for polymers experimentally is by using the onset of the absorption spectrum.[6,11] We compare calculated optical band gaps to experimental λ_{max} values for oligomers and to onset values for polymers. The experimental optical band gaps for the oligomers considered in this work were obtained from solution phase data. Regarding solvent effects, Seixas de Melo et al. found that the difference in optical absorption energies for a trimer and tetramer of furan measured in benzene and ethanol is roughly 0.06 eV.[79] (see Table S2 in the SI). This solvatochromism upon a sizable change in the dielectric constant between the polar and nonpolar solvent indicates that solvent corrections in the computations are not vital to study neutral oligomers. Alemán et al. investigated the influence of the polarity of the solvents on the orbital energy gap $\Delta\varepsilon$ of oligo/poly thiophene and their derivatives. These calculations also indicated that solvent effects can be neglected.[80]

Experimental IPs and EAs can be determined from high-resolution gas-phase ultraviolet photoelectron spectroscopy (UPS)[78,81] and photodetachment photoelectron spectroscopy (PD-PES),[77] respectively. Data for oligo-thiophenes are listed in SI Table S3. The band edge or "onset" of the first peak in PD-PES has been shown to agree reasonably well with calculated adiabatic EA values including zero-point vibrational energies ("0−0"). DFT/B3LYP differences between the 0−0 and vertical EAs were in the range of 0.01−0.04 eV[77] and are therefore sufficiently small for the larger oligomers studied herein that they can be neglected for semiquantitative comparisons with experiment. The IP values in the UPS experiments were obtained from Gaussian peak fitting. To be consistent with the EA data, we also list onset values and compare calculated vertical IP and EA data with experimental onset values.

2.3. Optimal Tuning. Part of this work is concerned with the application and ab initio optimization of RSE functionals. The following 3-parameter separation of the interelectronic distance r_{12} was utilized for the range separation of the interelectronic distance in the exchange[32]

$$\frac{1}{r_{12}} = \frac{1 - [\alpha + \beta\ \mathrm{erf}(\gamma r_{12})]}{r_{12}} + \frac{\alpha + \beta\ \mathrm{erf}(\gamma r_{12})}{r_{12}} \quad (1)$$

The second term on the right-hand side is used for the long-range eX component, and the first term is used for the short-range DFT component of the exchange. The parameter α quantifies the fraction of eX in the short-range limit, while $\alpha + \beta$ gives the fraction of eX in the long-range limit. The optimal tuning likely requires an asymptotically correct functional, i.e. $\alpha + \beta = 1$, for reasons discussed elsewhere.[55,64] The acronym LC is used to indicate a correct long-range behavior. We employed in its LC form a Perdew−Burke−Ernzerhof[82] hybrid (PBE0, $\alpha = 0.25$), since this functional has performed well in previous studies utilizing optimal tuning. The 25% eX in PBE0 can be justified based on first principles.[83]

dx.doi.org/10.1021/ct4009975 | J. Chem. Theory Comput. 2014, 10, 1035−1047

In eq 1, γ is the range separation parameter, representing the inverse of a cutoff range for the interelectronic separation around which the exchange functional switches from (predominantly) DFT to (predominantly) eX. Commonly used values for γ in globally parametrized functionals are in the range of 0.3 to 0.5. The PBE hybrid with $\alpha = 0.25$, $\gamma = 0.3$ is referred to in this work as LC-PBE0, while an optimally tuned version is indicated by the notation LC-PBE0*.

Optimal tuning is based on the finding that in exact Kohn−Sham (KS) and GKS theory, for an N-electron system the HOMO energy $\varepsilon_H(N)$ should be $-\mathrm{IP}(N)$ exactly.[84] With approximate functionals, however, the differences can be very large.[85] A more general discussion of the meaning of the HOMO and LUMO energies with different types of functionals can be found in ref 86. An optimal γ^* for an approximate functional with RSE is determined by minimizing $\varepsilon_H + \mathrm{IP}$ as best as possible both for a given N-electron molecule and possibly the corresponding $N \pm 1$-electron system. Following refs 64, 65, and 87−89, for the present work we minimized

$$J^2 = \sum_{i=0}^{1} [\varepsilon_H(N+i) + \mathrm{IP}(N+i)]^2 \tag{2}$$

which optimally tunes both HOMO(N) and the orbital corresponding to LUMO(N). As demonstrated in prior studies (see, for example, refs 46 and 48), the resulting functional typically achieves numerically very closely

$$\mathrm{IP}(N) \simeq -\varepsilon_H(N) \tag{3a}$$

$$\mathrm{EA}(N) \simeq -\varepsilon_L(N) \tag{3b}$$

The aforementioned curvature minimization is motivated by another exact condition, viz. that the correct molecular energy $E(N)$ as a function of N should afford straight-line segments[90] between integer N, with slopes corresponding to $-\mathrm{IP}$ of the species with next higher integer N. Deviations from the straight-line segment behavior indicates a DFT delocalization error (DE).[59] We found previously that for a given molecule and a given LC functional one can often find a continuum of γ^* values for different α, $\beta = 1 - \alpha$ that all satisfy an IP tuning criterion such as the one shown above.[64] Provided that the functional form and the parameter space in eq 1 is capable of delivering a vanishing DE, it is then possible to identify an optimal value for α (or β) nonempirically by requiring that the DE is as small as possible (referred to as "two-dimensional tuning" because two parameters and two criteria are optimized nonempirically). It was subsequently shown that the presence or lack of a derivative discontinuity is intimately related to the lack or presence of curvature in $E(N)$,[89] potentially indicating a path to further improvements. We note that RSE functionals often afford a smaller DE than standard functionals, and a "one-dimensional" IP tuning alone may already result in a very small DE. As is shown below, this is also the case for the oligomers studied herein.

Table S5 in the SI collects the optimal range-separation parameters and resulting J^2 values for varying numbers m of oligomer units up to a previously determined saturation limit.[62] The data were extrapolated to infinite m as indicated in the table footnote. These limiting values were also used for LC-PBE0* calculations on very long oligomers for which tuning calculations become rather resource-consuming.

2.4. Basis Size Effects. For the optimizations of the range-separation parameter γ, the basis set dependence was initially studied by employing the 6-31+G* and TZVP basis sets.[91,92] The difference between the optimal γ values from the two basis sets for the thiophene oligomers was only 0.002 bohr^{-1}. See Figure S2 and Table S5 in the SI. We conclude that with a valence basis set that would be considered as of acceptable quality for DFT applications the basis set dependence of γ^* can be neglected. The 6-31+G* parameter set was used for subsequent calculations.

Orbital energy gaps and optical gaps were computed from DFT and time-dependent DFT (TDDFT), respectively. Basis-size effects were examined again for the thiophene oligomers 2T, 4T, and 8T (See Figure S3 in the SI). The addition of diffuse or polarization functions beyond 6-31+G* changed the optical gaps by less than 0.01 eV and the orbital energies by less than 0.03 eV. Therefore, except in a few cases where explicitly stated otherwise, the 6-31+G* basis has been employed for subsequent oligomer calculations in order to keep the computational effort reasonably low overall. IP, EA, and fundamental gap values were also computed with 6-31+G* for consistency with the optical and orbital energy gaps.

2.5. Oligomers vs Infinite-Chain Polymers. Results of PBC calculations for polymers and corresponding oligomer calculations are collected in Table S4 of the SI. We compare here the HOMO and LUMO energies of relatively large oligomers with the corresponding energies of the "crystal orbitals" and their energy gaps. In agreement with previous work,[14] the calculated DFT orbital energy band gap occurs at the Γ point. The PBC data compare well with those for larger oligomers ($m \sim 20$ and higher), unlike data for oligomers with m significantly below 20. We therefore consider the oligomers used for the data in Table S4 to be reasonably close to the infinite-periodic limit. This allows us to investigate chain-length limits with functionals and certain parametrizations that are not yet available in the PBC code.

For the TDDFT calculations, the calculated vertical optical gap for 20T using the tuned LC-PBE0* functional is 2.10 eV. The result is in good agreement with an experimental range of 2.1 to 2.2 eV from the onset of the observed UV spectral band[93] (2.0 eV for a thin-film measurement.[94]) Additional data for different oligomer sizes calculated with the optimally tuned functionals are provided in SI Table S2. The lowest excitation energy changes from 2.10 eV (20T) to 2.07 eV (30T) to 2.04 eV (50T) with increasing m. Although there is a slight drop, one can consider the 20-mer to be reasonably close to the infinite-chain limit given the various approximations noted in section 2.2. An "effective conjugation length" has been defined by Meier et al.[95] where the wavelength of absorption maximum in a series of oligomers is not more than 1 nm from the infinitely long polymer chain value. Given the finite accuracy of the computations, and given the fact that 1 nm means different energies in different parts of the spectral range, a limiting effective conjugation for OT is approached past around $m = 20$. Using much shorter oligomers would be insufficient for predictions of the band gaps of conducting conjugated polymers such as PT.[16]

Experimentally, there is no substantial change in the excitation energies beyond 20T, while absorption intensities and conductivities keep increasing in going from 20T to 27T.[96] Our calculated oscillator strengths f increase with increasing oligomer size, from 8.11 (20T) to 12.6 (30T) and 21.7 (50T). For noninteracting monomers, f should be proportional to the monomer number m. For f/m, we find 0.41 (20T), 0.42 (30T), and 0.43 (50T), indicating that the absorption intensity is also

Table 1. Calculated Negative HOMO Energy $-\varepsilon_H$, LUMO Energy $-\varepsilon_{LUMO}$, IP, EA, Orbital Energy Gap $\Delta\varepsilon$, Fundamental Gap ΔE_F, and Optical Gap ΔE_O for 2T and 6T, along with Selected Experimental Data[a]

	HF	PBE	B3LYP	HSE	LC	LC*	expt
				2T			
$-\varepsilon_H$	7.70	5.06	5.74	5.58	8.26	7.72	
IP	6.41	7.42	7.49	7.51	7.85	7.72	7.75[b],7.95[c]
$-\varepsilon_L$	−1.54	2.18	1.61	1.83	−0.27	0.01	
EA	−0.81	−0.03	−0.05	−0.05	0.04	−0.01	0.049[d]
$\Delta\varepsilon$	9.24	2.88	4.13	3.75	8.53	7.71	
ΔE_F	7.22	7.45	7.54	7.56	7.81	7.73	7.70[e]
ΔE_O	4.22	3.72	3.87[f]	3.94	4.29	4.15	4.11[g]
				6T			
$-\varepsilon_H$	6.61	4.51	5.04	4.89	7.30	6.37	
IP	5.65	5.89	6.07	6.09	6.75	6.38	6.45[b],6.96[c]
$-\varepsilon_L$	−0.42	2.93	2.48	2.71	0.86	1.37	
EA	0.26	1.58	1.46	1.49	1.33	1.35	1.25[d]
$\Delta\varepsilon$	7.03	1.58	2.56	2.18	6.44	5.00	
ΔE_F	5.39	4.31	4.61	4.60	5.42	5.03	5.20[e]
ΔE_O	2.86	2.01	2.30[f]	2.31	2.95	2.63	2.87[g]

[a]All energies in electron volts. LC = LC-PBE0. [b]Onset values of first peak in UPS collected from refs 78 and 81, with uncertainties of ±0.05 eV. [c]Peak values obtained by fitting Gaussian function, refs 78 and 81. [d]Onset values of the first peak in PD-PES, ref 77. [e]Difference between experimental IP and EA. [f]The TDDFT optical gaps ΔE_O of 2T and 6T calculated with the PBE0 global hybrid are 3.96 and 2.40 eV, respectively. [g]Maximum of absorption in $CHCl_3$.[20,99] See details in SI Table S2.

sufficiently well converged past m = 20. In the following discussion, results from sufficiently large oligomers are used in place of the infinite-chain limits due to the limited selection of functionals and lack of TDDFT excitation energies in the PBC code.

3. RESULTS AND DISCUSSION

Calculated energy gaps obtained with HF and DFT are assessed first. A discussion of IP and EA values follows. The data set includes results from the optimally tuned LC-PBE0*. Details on the tuning results and the delocalization error (DE) are provided in section 3.2. Finally, the frontier molecular orbitals and the possibility of charge-transfer (CT) character in the electronic excitations are investigated.

3.1. Band Gaps, IP, and EA. A band gap of an extended periodic system is often defined as the difference between the lowest energy in the conduction band and the highest energy in the valence band.[35] This short definition is based on a theory invoking some type of one-electron property or quasi-particle property, such as orbital energies and their analogs in extended periodic systems. It is certainly possible to define quasi-particles ("orbitals") from many-body theory with associated energies that correspond to observable energies or energy gaps, along with practical approximations that deliver good accuracy in computations. For example, quasiparticle energy spectra from "GW" calculations can produce reasonable energy gaps for solids or electron attachment/detachment energies for molecules.[29,65,97,98] As pointed out in the Introduction, one type of calculated energy gap cannot simultaneously refer to different experimentally observable quantities. Moreover, practical calculations rely on approximations. For instance, as discussed above the exact Kohn−Sham density functional would produce $IP(N) = -\varepsilon_H(N)$. However, approximate functionals do not typically deliver this result. Further, except when it is achieved fortuitously or via optimal tuning, with approximate functionals $\Delta\varepsilon$ does not correspond to the optical or the fundamental gap.

Table 1 collects various energy gaps, orbital energies, as well as IP and EA data, for the thiophene dimer and hexamer (2T, 6T). Experimental data, where applicable, are also shown. Among HF theory and different hybrid and nonhybrid functionals, the orbital energy gap $\Delta\varepsilon$ ranges from 2.9 to 9.2 eV for 2T, and from 1.6 to 7.0 eV for 6T. The optical gaps ΔE_O, calculated as vertical TDDFT (or TDHF) excitation energies, vary considerably less. HF and the nontuned LC-PBE0 give ΔE_O somewhat above experiment, PBE and B3LYP are significantly too low, and the optimally tuned LC-PBE0* produces optical gaps that are close to experiment. For these two oligothiophenes as well as longer oligomers (SI Table S1) the $\Delta\varepsilon$ values from the B3LYP calculations are not far from the ΔE_O from LC-PBE0* as well as experiment. This is clearly coincidental, since $\Delta\varepsilon$ varies by many electron volts depending on the fraction of eX in the functional. Previous work[16,35,102] correlated calculated orbital energy gaps for oligo-thiophene, -pyrrole, -paraphenylene, and -furane with experimental optical gaps. For instance, in some cases B3LYP $\Delta\varepsilon$ values produced reasonable agreement with experimental ΔE_O for selected oligomer sizes, but—as in the present work—the agreement is somewhat fortuitous. The B3LYP TDDFT optical gaps are too low in comparison.

As with the optical gap, the fundamental gaps (calculated from total energy differences) vary much less than $\Delta\varepsilon$ among the various methods. In comparison, $\Delta\varepsilon$ is much smaller than ΔE_F for PBE and B3LYP and considerably larger than ΔE_F with LC-PBE0 and HF. For the optimally tuned LC-PBE0*, $\Delta\varepsilon$ is—by construction—in excellent agreement with the calculated ΔE_F. Likewise, for the optimally tuned functional the HOMO energy agrees well with −IP and the LUMO energy with −EA. The agreement of the LC-PBE0* results with experimental data is also reasonable for the IPs and EAs. The optical energy gaps for small oligomers of thiophene calculated from the tuned functional also compare acceptably well with results from correlated wave function based quantum chemistry methods. Numerical data are provided in Tables S1 and S2 in the SI. We note that the scaling of correlated wave function methods with

the number of basis functions is high, currently preventing routine calculations on significantly larger systems.

The individual IP and EA data are listed in Table 1, and differences with respect to the experimental data for 6T are shown in Figure 2. For the functional PBE (nonhybrid) and

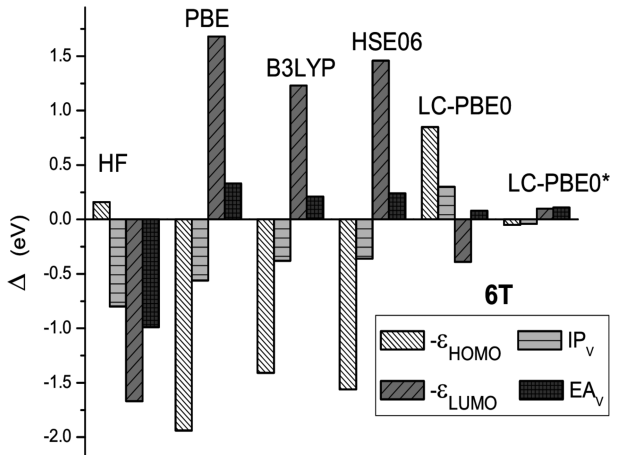

Figure 2. (6T) Differences (Δ) between the calculated orbital energies ($-\varepsilon_{HOMO}$, $-\varepsilon_{LUMO}$) and calculated vertical IP and EA with respect to the "onset" experimental IP (6.45 eV) and EA (1.25 eV).

B3LYP (global hybrid) the negative orbital energies, $-\varepsilon_{HOMO}$ and $-\varepsilon_{LUMO}$, are far from the calculated IP and EA (obtained from total energy differences of the N and $N \pm 1$ electron systems). Compared to the corresponding experimental IP and EA, PBE, and B3LYP produce too low $-\varepsilon_{HOMO}$ and too high $-\varepsilon_{LUMO}$, along with a small orbital energy gap $\Delta\varepsilon$. The IP and EA values calculated from total energy differences, however, agree reasonably well with those from the RSE functionals (nontuned and optimally tuned). Per Koopmans' theorem, $-\varepsilon_H$ from the HF calculations should be a reasonable approximation to the IP. The data show that the approximation is in fact quite poor when the comparison is made with the IP calculated with HF from $E(N-1) - E(N)$. Interestingly, though, both for 2T and 6T the HF $-\varepsilon_H$ value is not far from the experimental IP. However, this agreement is likely fortuitous. The HF $-\varepsilon_{LUMO}$ is also seen to be a poor approximation of the EA. Extrapolations using HF data would not be reliable in order to draw conclusions about any of the energy gaps. In contrast, with DFT the optimally tuned functionals perform satisfactorily for all the calculated parameters.

Regarding the long-range screened HSE functional, the various energies and energy gaps in Table 1 are mostly bracketed by PBE and B3LYP. The HSE orbital energy gap, $\Delta\varepsilon$, is smaller but quite close to the B3LYP TDDFT optical gap, also for larger oligomers (SI Table S1). This trend is consistent with ref 68, where it was found that the HSE orbital energy gap was close to the TDDFT optical gap calculated with the corresponding unscreened global hybrid, which would be the PBE0 hybrid functional. Typically, B3LYP (20% eX) and PBE0 (25% eX) perform similar in TDDFT calculations; as the data in the footnotes of Table 1 show, the PBE0 optical gaps for 2T and 6T are indeed close to B3LYP, about 0.1 eV larger. However, as already pointed out B3LYP (and PBE0, to a slightly lesser degree) underestimates the optical gap with TDDFT when compared with the optimally tuned LC functional and experiment, while $\Delta\varepsilon$ is fortuitously close to ΔE_O obtained with the optimally tuned functionals. These findings echo the somewhat better agreement of B3LYP orbital energy gaps with experimental optical gaps, as compared to HSE, for one-dimensional extended π-conjugated systems noted in various other studies,[103,104] notwithstanding the generally good performance of HSE in calculations on three-dimensional periodic systems. The trends in Tables 1 and S1 also exhibit the aforementioned effect of $\Delta\varepsilon$ numerically approaching ΔE_O for increasing system size for the semilocal PBE functional.

Figure 3 shows a comparison of calculated vertical fundamental and optical gaps of oligo- and polythiophene

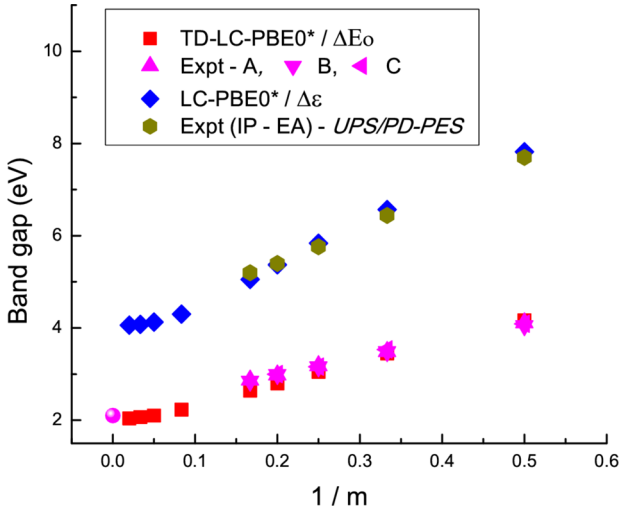

Figure 3. Calculated orbital energy gap $\Delta\varepsilon$ and optical gap of mono-, oligo-, and polythiophene using an optimally tuned RSE functional vs the reciprocal of the number of monomer units ($1/m$). Numerical data are provided in the SI. By construction, $\Delta\varepsilon \simeq \Delta E_F$. Experimental data as follows: (optical gap) A = maximum of absorption, $CHCl_3$ solvent.[20,99] B = dioxane solvent.[100] C = CH_3CN solvent.[79] (fundamental gap) UPS/PD-PES = difference between experimental IP and EA.[77,78,81,101] (polymer data). References 93 and 94.

with experimental data, as a function of $1/m$. The optimally tuned functional LC-PBE0* was used for the comparison. Overall, the agreement is quite reasonable as far as the trends and the large difference between ΔE_F and ΔE_O are concerned. To verify that the good performance of the optimal tuning for polythiophene (PT) is not a coincidence, we also performed calculations of band gaps on two other types of conjugated systems, PE and PF (Figure 1), see Table 2. The optical gaps calculated for 20F (2.44 eV) and 30F (2.40 eV) are close to the experimental value of 2.35 eV for PF.[106] The optical gaps for 15EDOT, 20EDOT, and 30EDOT agree well with the experimental optical bandgap, reported to be in the range of 1.6−1.9 eV.[15,105]

3.2. Delocalization Error. Many important properties of a conjugated polymer and large oligomers depend on the extent of conjugation and the extent of physically meaningful delocalization of π orbitals along the conjugated backbone. The concept of bond-length alternation (BLA) is often invoked in order to gauge the degree of delocalization,[107] but other criteria such as the extent of delocalization of localized π orbitals can also be used.[48] The BLA criterion has the advantage that it is accessible by experiment as long as reliable structural data are available. However, the DE may affect BLA in optimized geometries less than other properties such as

dx.doi.org/10.1021/ct4009975 | J. Chem. Theory Comput. 2014, 10, 1035−1047

Table 2. Comparison between Experimental and Calculated Optical Gaps (eV) for PT, PE, and PF Using Optimally Tuned LC-PBE0* Functionals: 6-31+G* Basis[a]

	20T	30T	50T	expt PT
ΔE_O	2.10	2.07	2.04	2.1−2.2, 2.0[b]
	15E	20E	30E	expt PE
ΔE_O	1.98	1.92	1.87	1.6−1.9[c]
	15F	20F	30F	expt PF
ΔE_O	2.50	2.44	2.40	2.35[d]

[a]Slow convergence of the TDDFT calculations for 30T, 50T, 30E, and 30F with the 6-31+G* basis. The listed values were obtained with TDDFT using the 6-31G* basis and adding the differences of corresponding $\Delta\varepsilon$ between 6-31+G* and 6-31G*. Figure S3 in the SI shows that the basis set effects on $\Delta\varepsilon$ and ΔE_O are very similar and, furthermore, become smaller for increasing oligomer lengths. [b]2.1−2.2 eV: onsets of the observed spectral band. 2.0 eV: thin-film measurement.[93,94] [c]Reference 15 and 105. [d]Reference 106.

optical gaps,[108] while in turn functionals with small DEs may not predict the most physically reasonable BLA.[109]

Here, we take the opportunity to probe the DFT delocalization error (DE) directly, numerically, in the calculations. As pointed out already, the sign and relative magnitude of the DE is indicated by the sign and extent of curvature (deviation from straight-line segments) when the energy, $E(N)$, of a molecule is calculated as a function of fractional electron number N. In previous work on conjugated "push−pull" chromophores,[48] we have argued that that a vanishing DE does not imply vanishing delocalization, but rather it indicates a vanishing *unphysical* delocalization. Similar considerations apply to conjugated polymers.

It was further noted in prior work that for conjugated π systems the optimally tuned range-separation parameter γ^* decreases with increasing chain lengths,[48,61,62,65] meaning that in systems with spatially more extended conjugation (longer range delocalization) the switch to eX occurs at larger interelectronic distances (γ is in inverse length units). Its inverse has been associated with the spatial extent of electronic coupling.[62] One may therefore also correlate different values of γ^* for different oligomer sizes with the effective conjugation length mentioned above. For oligo-thiophene, optimal values of the range-separation parameter (γ^*), and the resulting J^2 values of practically zero, are collected in Table S5 and Figure S2 in the SI. As the monomer number m increases, γ^* decreases—as expected—and converges to a value of 0.093 au for long chains.

Figure 4a shows the fraction of eX in the various functionals versus the interelectronic distance r_{12}. A plot corresponding to the optimally tuned LC-PBE0* for 6T is also included. For 6T, the tuned functional affords roughly 3/4 eX, 1/4 DFT exchange, at r_{12} around 6 atomic units (which is roughly twice a C−C single-bond distance), while LC-PBE0 with a more commonly applied γ of 0.3 already gives almost 100% eX. The functional is therefore overall very HF-like in the exchange component for 6T and larger oligomers. At first look, this may seem irrelevant as there is still a DFT correlation component. However, the balance of DFT exchange and correlation in approximate functionals, and an accompanying self-interaction, in fact covers certain aspects of the electron correlation. This is one of the reasons why global hybrid functionals with large fractions of eX are usually not performing well for thermochemistry.[110]

Regarding the (optimal) γ^* values for different polymer systems (see Table S5 in SI), the limiting γ^* of PT (0.093) is larger than that of PE (0.078) and smaller than that of PF (0.109). This is in accord with a finding by Zade and Bendikov[16] that PT has lower degree of conjugation than PE and higher degree than PF. Therefore, as was pointed out also in ref 62, it is reasonable to present $1/\gamma^*$ as an indicator of the spatial extension of physically meaningful delocalization, i.e. a measure of conjugation length.

Next, we examine the behavior of $E(\Delta N)$ for 2T, 6T, and 12T as representative examples from our test set. Figure 4b

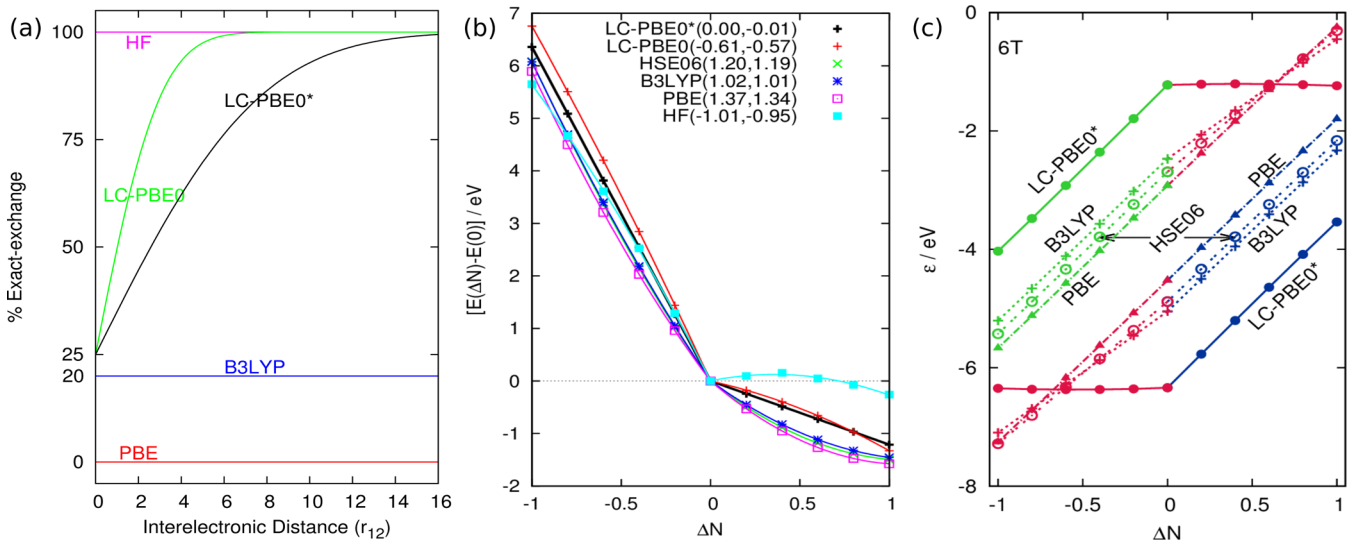

Figure 4. (a) Percentage of eX included as a function of interelectronic distance for the various functionals. Tuned variant (γ^*) for 6T. (b) Energy of 6T as a function of fractional electron number, ΔN, relative to neutral system ($\Delta N = 0$). The numerical values in the plot correspond to the coefficients of $(\Delta N)^2$ of quadratic fits to $E(N)$ in the electron-deficient and electron-rich regime, respectively ($\Delta N < 0$, $\Delta N > 0$). Similar plots for 2T and 12T are provided in Figure S4 in the SI. (c) Molecular orbital energies (eV) for the frontier orbitals of 6T calculated with fractional electron numbers ΔN, relative to the neutral systems. The electron deficient part of each plot shows the HOMO (red) and LUMO (green) energies; the electron-rich part shows the HOMO-1 (blue) and HOMO (red) energies.

dx.doi.org/10.1021/ct4009975 | J. Chem. Theory Comput. 2014, 10, 1035−1047

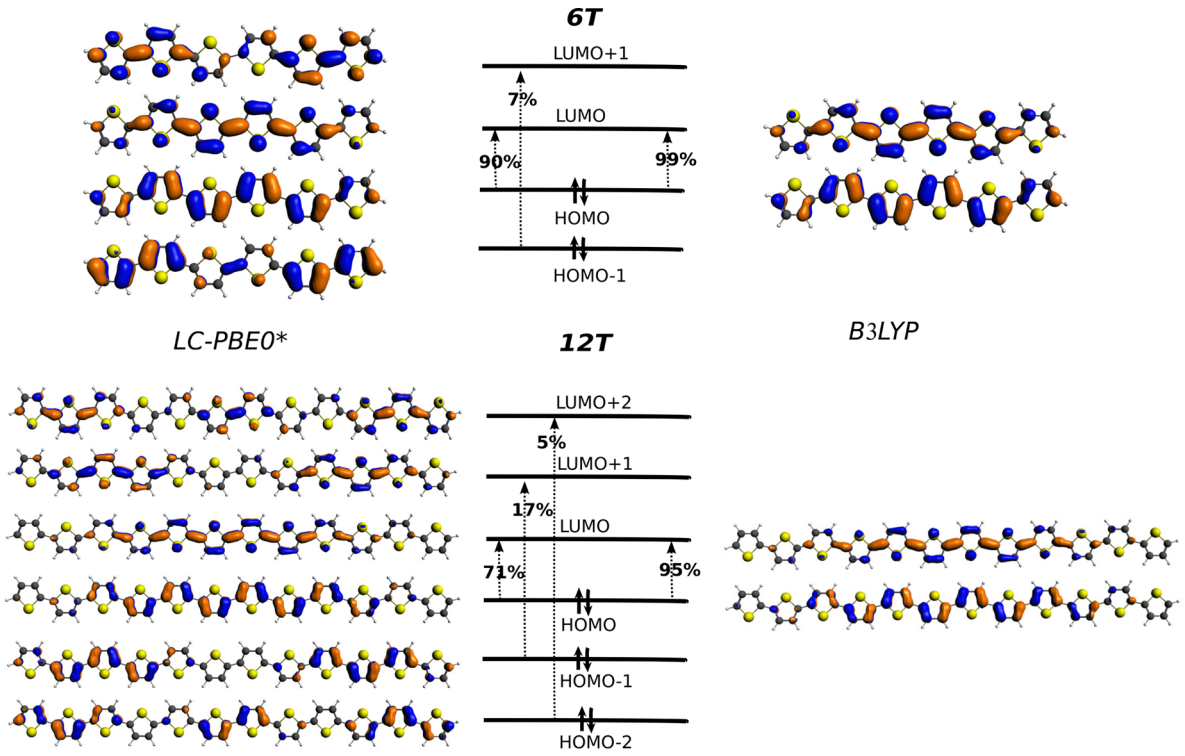

Figure 5. Occupied−unoccupied orbital pair contributions to the lowest-energy singlet transition, from TDDFT data for 6T and 12T using the LC-PBE0* and B3LYP functionals (6-31+G* basis). Isosurface values are ±0.03 au for the orbital plots.

shows calculated energies for 6T as a function of N around the electron number for the neutral molecule, along with second-order polynomial fits to the data. The coefficients of $(\Delta N)^2$, indicating the presence of absence of curvature, are provided separately for $\Delta N < 0$ and $\Delta N > 0$. Similar plots for 2T and 12T are given in Figure S4 in SI. Positive curvature indicates too much, and negative curvature indicates too little, delocalization. The negative curvature of $E(\Delta N)$ from the HF calculations is quite typical and indicative of insufficient delocalization. As in our previous paper,[48] some of the HF data points afford numerical noise due to poor SCF convergence, but the trend is evident. The nonhybrid functional PBE gives much too strong delocalization as indicated by the positive curvature of $E(\Delta N)$. This DE goes along with significant underestimations of the optical gaps in the TDDFT calculations discussed in section 3.3. B3LYP produces less delocalization error than PBE, but the curvatures values remain large. In line with the trends in Table 1, the delocalization error for HSE is in between B3LYP and PBE, which is not surprising as the functional switches from a 25% hybrid in short-range to pure PBE at long-range. The nontuned LC-PBE0 produces negative curvature of $E(\Delta N)$, but significantly less so than HF. From 2T to 12T, the optimally tuned LC-PBE0* variants produce very small $E(\Delta N)$ curvatures (Figures 4b and S4 and Table S4 (SI)). Since the performance of the LC-PBE0* calculations is very reasonable, additional curvature minimization as performed in ref 64 is unlikely to improve the results significantly. We therefore decided to forego a computationally more expensive two-dimensional tuning.

Figure 4c shows the dependence of the frontier orbital energies of 6T as a function of electron number N. The plot is representative of the different oligomers studied in this work. The PBE orbital energies vary approximately linearly with N, reflecting the curvature and lack of derivative discontinuity in $E(\Delta N)$. For the optimally tuned LC functional, the HOMO energies are constant between integers, corresponding to the slopes of $-E(\Delta N)$ segments in Figure 4b. This is the expected correct behavior. At integer N, a different orbital becomes the HOMO. As seen in the plot, the LUMO energy of the system with a fractional hole ($\Delta N < 0$) connects continuously to the HOMO energy of the system with a fractional extra electron. As the HOMO energies in both plot regimes are physically meaningful, at $\Delta N = 0$ we have the desired result of $\Delta\varepsilon = \Delta E_F$. For comparison, the orbital energies of 6T are also shown for B3LYP and HSE in Figure 4c, indicating a noticeable, but small, qualitative change from the PBE toward the LC-PBE0* behavior.

To summarize this subsection: The curvature of $E(\Delta N)$ and the behavior of the frontier orbital energies as a function of fractional electron number serve as an excellent diagnostics for the problems with calculating band gaps with HF and nonhybrid functionals for the set of polymer systems. The inverse of the optimal γ^* appears to be a suitable indicator of the spatial extent of the conjugation at different oligomer lengths.

3.3. Analysis of the Electronic Excitations. This last subsection of the discussion focuses on the optical gaps calculated by TDDFT, the nature of the lowest-energy electronic singlet excitations, and to which extent known problems of GGA and global hybrid functionals to predict charge-transfer (CT) and "CT-like" excitations[88] influence the quality of the results.

An excitation in TDDFT can be assigned by considering the weights by which different pairs of occupied and unoccupied orbitals ("occ−unocc") contribute to the transition density. As shown in Figure 5, functionals with low fractions of eX give an almost pure HOMO−LUMO transition. With eX-rich func-

dx.doi.org/10.1021/ct4009975 | J. Chem. Theory Comput. 2014, 10, 1035−1047

tionals the excitations involves other MO pairs but remains HOMO−LUMO dominant. In the TDDFT linear response equations for excitation energies, the HOMO−LUMO orbital energy gap $\Delta\varepsilon$ then serves as a rough estimate of ΔE_O. A qualitative distinction among the functionals in Table 1 was already pointed out: for PBE the TDDFT excitation energy is larger than $\Delta\varepsilon$; whereas for the LC functionals and HF (where $\Delta\varepsilon$ approximates or represents the fundamental gap) the TDDFT excitation energy is smaller than $\Delta\varepsilon$. For B3LYP, ΔE_O and $\Delta\varepsilon$ are fortuitously close to each other with $\Delta\varepsilon \gtrsim \Delta E_O$. For 6T and longer chains, the excessively small $\Delta\varepsilon$ of PBE in conjunction with the small admixture of other orbital pairs renders the calculated optical gaps much too low. For the eX rich functionals, mixing of different occ−unocc orbital pairs is fundamentally needed to describe the electronic transition for the reason that the HOMO and LUMO approximate, or represent, electron detachment/attachment rather than an excitation.

Next, consider the relation between the optical gaps and fundamental gaps. Time-dependent HF perturbation theory for a two-orbital model involving only the HOMO and the LUMO of an oligomer gives for the energy of a singlet excitation

$$\Delta E_O = \Delta\varepsilon - J + 2K \tag{4a}$$

where J and K are the Coulomb and exchange electron repulsion integrals calculated with the two orbitals. It is important to note that J in the excitation energy stems from the *exchange* term in the HF potential. For a CT excitation between spatially nonoverlapping orbitals at large distance $\boldsymbol{R}$ one expects[46,81,111,112] ("Mulliken rule", in atomic units)

$$\Delta E_O = \mathrm{IP} - \mathrm{EA} - 1/R \tag{4b}$$

and $K \approx 0$. An optimally tuned LC functional can clearly deliver this behavior:[112,113] With a large distance separating HOMO and LUMO, DFT exchange-correlation terms in the TDDFT excitation expression become negligible, the LR exchange gives $J \to 1/R$ from eq 4a, while at the same time $\Delta\varepsilon = \Delta E_F = \mathrm{IP}$ — EA from the tuning. In most situations—and certainly for the oligomers studied herein—however, the HOMO and LUMO are not spatially separated. Consequently, one would not expect a behavior of the optical gap following eq 4b.

Figure 6, displays plots for oligothiophene of $\Delta\varepsilon - \Delta E_O$ as well as $1/R$ versus $1/m$. Here, a measure for R was taken to be the distance between the two carbon atoms at the opposite ends of an oligomer chain, and $1/R$ in atomic units was converted to an energy. For an optimally tuned functional, eq 4b would give $\Delta\varepsilon - \Delta E_O = (\mathrm{IP} - \mathrm{EA}) - \Delta E_O = +1/R$. Interestingly, apart from a global offset of the LC-PBE0* data points, their plot follows roughly the same slope as $1/R$ for m up to about 12. The other functionals do not exhibit the same parallel trend to $1/R$ (with B3LYP, PBE, and HSE giving a negative slope), but we have already seen that they neither afford $\Delta\varepsilon = \mathrm{IP} - \mathrm{EA}$ nor do they produce particularly accurate optical gaps for oligothiophenes. The apparent $1/R$ component in the LC-PBE0* excitation energies made us wonder whether the excitations afford a CT-like character.

CT character of an excitation with a dominant contribution from an occ−unocc orbital pair ϕ_p, ϕ_q can be assessed with the help of spatial overlaps,[85,114,115] for example (assuming real orbitals)

$$O_{p,q} = \langle|\phi_p||\phi_q|\rangle = \int |\phi_p(\mathbf{r})||\phi_q(\mathbf{r})|\,\mathrm{d}V \tag{5}$$

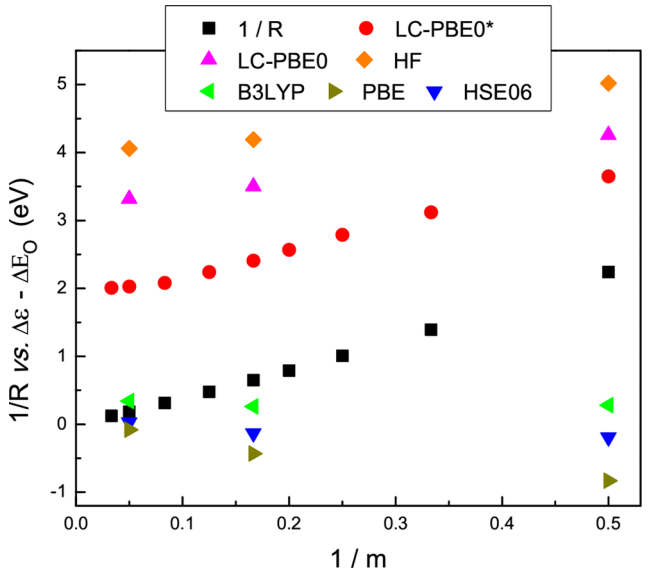

Figure 6. Oligothiophene: Difference between orbital energy gap and optical gap calculated with different functionals, versus inverse monomer number. $\boldsymbol{R}$ is approximately the oligomer chain length (separation of the two most distant carbons). $1/\boldsymbol{R}$ in atomic units has been converted to an energy in electron volts and is also shown.

Here, $|\phi_p(\boldsymbol{r})| = [\phi_p(\boldsymbol{r})\phi_p(\boldsymbol{r})]^{1/2}$ is the absolute value (modulus) of an orbital ϕ_p at a given point in space, and $0 \le O_{p,q} \le 1$. Since the MOs are orthogonal by construction, the usual overlap integral do not provide this kind of information. A small spatial overlap, for instance $O_{H,L}$ between the HOMO and the LUMO being below approximately 0.5, may indicate sizable CT, which then typically leads to dramatically too low excitation energies in calculations with nonhybrid functionals such as PBE and, to a lesser extent, with hybrids such as B3LYP. RSE functionals can overcome this problem. For organic π-chromophores there are also "CT-like" HOMO−LUMO transitions, for which Kuritz et al. used the following criterion for symmetric molecules:[88] Define

$$\phi_a = (\phi_H + \phi_L)/\sqrt{2}$$
$$\phi_b = (\phi_H - \phi_L)/\sqrt{2} \tag{6}$$

and calculate the spatial overlap $O_{a,b}$. A small $O_{a,b}$ was thought to indicate an involvement of spatially distant orbitals and a CT-like problem, even if $O_{H,L}$ is large. The excitation energy would then be expected to improve with an RSE functional and further benefit from optimal tuning. Equation 6 can be understood as a special case of an orthogonal transformation with a 45° angle and one may have to consider other angles to detect a small overlap. Qualitatively, it is clear that for a pair of spatially extended orbitals with somewhat comparable local nodal patterns, but with one of them being odd and the other one being of even parity with respect to reflection or inversion at the molecular center, $O_{H,L}$ can potentially be large while at the same time $O_{a,b}$ of eq 6 can be small. The HOMO−LUMO pair of 12T in Figure 5, for instance, indicates such odd and even character with respect to the inversion center.

Figure 7 displays the relevant orbitals ϕ_a, ϕ_b for the 2T, 6T, and 12T systems, along with the spatial overlap values for the HOMO−LUMO pair and the corresponding combinations per eq 6. Numerical data for oligomers of thiophene, furane, and ethylenedioxythiophene with m up to 20 are collected in Table

dx.doi.org/10.1021/ct4009975 | J. Chem. Theory Comput. 2014, 10, 1035−1047

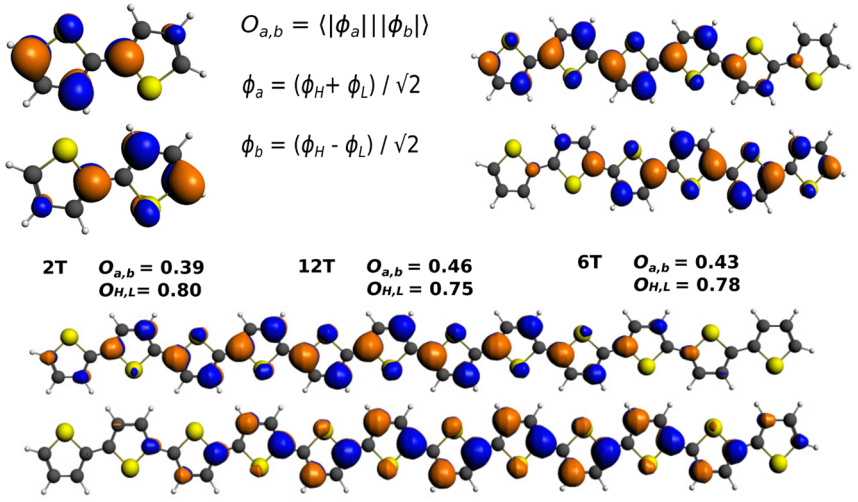

Figure 7. Orbital plots of the normalized sum and difference of HOMO and LUMO orbitals for 2T, 6T, and 12T, as obtained from the optimally tuned LC-PBE0* functional.

3. The overlaps were obtained from numerical integrations on regular Cartesian grids with 10^6 points, giving a precision of 0.01 or better. For the 20-mer of each compound, Figure 8 shows the spatial overlap of linear combinations of the HOMO and LUMO corresponding to orthogonal rotations at varying angles, with 45° corresponding to Table 3. The figure demonstrates that the lowest spatial overlaps are found for the latter case. Furthermore, for all oligomers it is indeed found that, while the spatial overlaps of HOMO and LUMO are not small (0.74 and above), those of the linear combinations level off below 0.50 for increasing chain length. Accordingly, based on the criterion from ref 88, one may cautiously assign a certain character of CT to the longest-wavelength electronic transitions of the oligomers studied in this work.

Table 3. Spatial Overlaps $O_{H,L}$ and $O_{a,b}$, with a,b Defined in Equation 6, for Selected m-mers of PT, PE, and PF: LC-PBE0* Functional

m-T	2T	6T	12T	20T
$O_{H,L}$	0.80	0.78	0.75	0.74
$O_{a,b}$	0.39	0.43	0.46	0.48
m-E	2E	6E	15E	20E
$O_{H,L}$	0.82	0.80	0.78	0.77
$O_{a,b}$	0.39	0.41	0.45	0.46
m-F	2F	6F	15F	20F
$O_{H,L}$	0.80	0.78	0.76	0.75
$O_{a,b}$	0.40	0.43	0.47	0.48

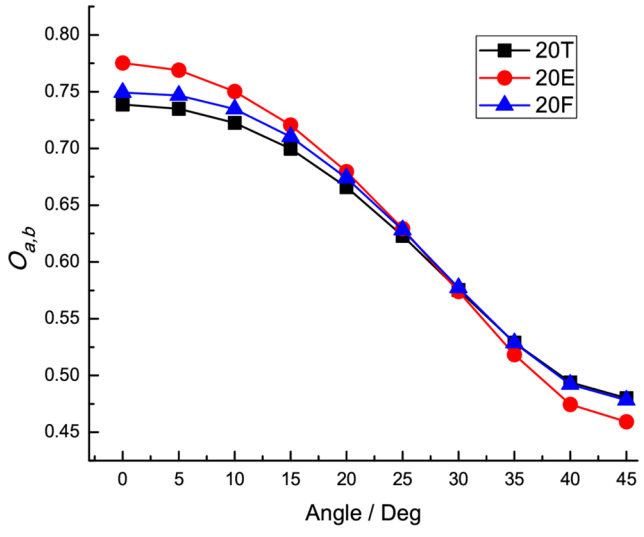

Figure 8. Spatial overlaps $O_{a,b}$ for $\phi_a = \phi_H s + \phi_L c$, $\phi_b = \phi_H c - \phi_L s$ with $c = \cos\alpha$, $s = \sin\alpha$, versus α (deg) for 20T, 20E, and 20F. Equation 6 corresponds to $\alpha = 45°$: LC-PBE0* functional.

Very recently, Guido et al. suggested a new descriptor for CT character of an excitation in TDFFT calculations. This descriptor is based on a weighted sum of distances between the centroids, $R_{pq} = |\langle\phi_p|\mathbf{r}|\phi_p\rangle - \langle\phi_q|\mathbf{r}|\phi_q\rangle|$, of pairs of orbitals such as p = HOMO, q = LUMO, involved in the excitation.[116] The required data are easily computed as only dipole integrals are needed. In ref 116, a weighted sum of less than 1.5 Å indicated short-range excitations for which traditional GGA and hybrid functionals performed reasonably well. However, this descriptor does not work for our samples because, due to the symmetry, the orbital centroids are all located at or very close to the center of mass. It is, however, possible that a CT-like character would be revealed by application of the centroid criterion to the linear combinations of eq 6. We plan to investigate this possibility in the near future, as further work on diagnosing CT-like excitations is ongoing in our group.

4. SUMMARY AND CONCLUSIONS

Optical and fundamental band gaps, as well as IP and EA, of selected π-conjugated organic oligomers and polymers are well described computationally with tuned RSE hybrid functionals. By construction, the HOMO−LUMO orbital energy gap $\Delta\varepsilon$ is equal to IP−EA in such calculations while the optical gap is typically much smaller. Optimal range-separation parameters for polymers can be obtained via oligomeric extrapolation from calculations on finite systems where the IP is easily calculated from ground state energy differences obtained with different electron numbers. Numerical examples show that previously reported agreement of B3LYP $\Delta\varepsilon$ with measured optical gaps is somewhat fortuitous and therefore not likely to perform uniformly well for a diverse set of polymer systems or for a large range of oligomer lengths. With the help of numerical

dx.doi.org/10.1021/ct4009975 | J. Chem. Theory Comput. 2014, 10, 1035−1047

examples, this work wishes to reiterate that "band gaps" may refer to different observable quantities and that $\Delta\epsilon$ gaps calculated with DFT more often than not represent none of the experimentally observable energy gaps numerically. For the oligomer systems studied herein, the lowest-energy electronic excitations are assigned as HOMO−LUMO π-to-π^*. Nevertheless, the spatial overlaps of frontier molecular orbitals and linear combinations thereof indicate the possibility of a "CT-like" character. In such a situation, an improved performance of RSE hybrid functionals for the optical gaps, in particular when optimally tuned, can be expected.

■ ASSOCIATED CONTENT

Supporting Information

Optimal range-separation parameters for thiophene oligomers (OT), calculated with LC-PBE0*/6-31+G*. Basis size effects for the calculated parameters and properties of selected oligomers, with the optimally tuned functional LC-PBE0*. Optical gaps, oscillator strength, and contribution of the HOMO−LUMO product to the lowest-energy allowed electronic transition calculated with different functionals for selected oligomers. Results from PBC calculations for polymers using G09 compared with corresponding oligomer results obtained with NWChem. J^2 values for the interpolated optimal γ^*. Additional graphical and numerical data for the analysis of DEs for selected oligomers. This material is available free of charge via the Internet at http://pubs.acs.org.

■ AUTHOR INFORMATION

Corresponding Author

*E-mail: jochena@buffalo.edu.

Notes

The authors declare no competing financial interest.

■ ACKNOWLEDGMENTS

We would like to thank the Center for Computational Research (CCR) at the University at Buffalo for providing computational resources. HS gratefully acknowledges financial support of the China Scholarship Council. J.A. acknowledges support from grants CHE-0952253 and CHE-1265833 of the National Science Foundation.

■ REFERENCES

(1) Inzelt, G. *Conducting Polymers: A New Era in Electrochemistry*; Scholz, F., Ed.; Monographs in Electrochemistry; Springer: Berlin Heidelberg, 2008; Chapter 1, pp 1−6.
(2) Skotheim, T., Elsenbaumer, R., Reynolds, J., Eds.; *Handbook of Conducting Polymers*, 2nd ed.; Marcel Dekker, Inc.: New York, 1998.
(3) Roncali, J. *Chem. Rev.* **1992**, *92*, 711−738.
(4) Roncali, J. *Chem. Rev.* **1997**, *97*, 173−206.
(5) Greenham, N. C.; Moratti, S. C.; Bradley, D. D. C.; Friend, R. H.; Holmes, A. B. *Nature* **1993**, *365*, 628−630.
(6) Gierschner, J.; Cornil, J.; Egelhaaf, H.-J. *Adv. Mater.* **2007**, *19*, 173−191.
(7) Moore, E. E.; Yaron, D. *J. Phys. Chem. A* **2002**, *106*, 5339−5347.
(8) Jones, B. A.; Facchetti, A.; Wasielewski, M. R.; Marks, T. J. *J. Am. Chem. Soc.* **2007**, *129*, 15259−15278.
(9) Kohler, A.; dos Santos, D. A.; Beljonne, D.; Shuai, Z.; Bredas, J.-L.; Holmes, A. B.; Kraus, A.; Mullen, K.; Friend, R. H. *Nature* **1998**, *392*, 903−906.
(10) Brédas, J.-L.; Cornil, J.; Beljonne, D.; dos Santos, D. A.; Shuai, Z. *Acc. Chem. Res.* **1999**, *32*, 267−276.
(11) Salzner, U.; Lagowski, J.; Pickup, P.; Poirier, R. *Synth. Met.* **1998**, *96*, 177−189.
(12) Salzner, U.; Pickup, P. G.; Poirier, R. A.; Lagowski, J. B. *J. Phys. Chem. A* **1998**, *102*, 2572−2578.
(13) Telesca, R.; Bolink, H.; Yunoki, S.; Hadziioannou, G.; Van Duijnen, P. T.; Snijders, J. G.; Jonkman, H. T.; Sawatzky, G. A. *Phys. Rev. B* **2001**, *63*, 155112.
(14) Hutchison, G. R.; Zhao, Y.-J.; Delley, B.; Freeman, A. J.; Ratner, M. A.; Marks, T. J. *Phys. Rev. B* **2003**, *68*, 035204.
(15) Torras, J.; Casanovas, J.; Alemán, C. *J. Phys. Chem. A* **2012**, *116*, 7571−7583.
(16) Zade, S. S.; Bendikov, M. *Org. Lett.* **2006**, *8*, 5243−5246.
(17) Izmaylov, A. F.; Scuseria, G. E. *J. Chem. Phys.* **2008**, *129*, 034101.
(18) Pappenfus, T. M.; Schmidt, J. A.; Koehn, R. E.; Alia, J. D. *Macromolecules* **2011**, *44*, 2354−2357.
(19) Cornil, J.; Beljonne, D.; Brédas, J. L. *J. Chem. Phys.* **1995**, *103*, 834−841.
(20) Hutchison, G. R.; Ratner, M. A.; Marks, T. J. *J. Phys. Chem. A* **2002**, *106*, 10596−10605.
(21) Fabiano, E.; Sala, F. D.; Cingolani, R.; Weimer, M.; GÃűrling, A. *J. Phys. Chem. A* **2005**, *109*, 3078−3085.
(22) Rubio, M.; Merchán, M.; Pou-AméRigo, R.; Ortí, E. *ChemPhysChem* **2003**, *4*, 1308−1315.
(23) Rubio, M.; Merchán, M.; Ortí, E. *ChemPhysChem* **2005**, *6*, 1357−1368.
(24) Ye, A.; Shuai, Z.; Kwon, O.; Brédas, J. L.; Beljonne, D. *J. Chem. Phys.* **2004**, *121*, 5567−5578.
(25) Chen, L.; Zhu, L.; Shuai, Z. *J. Phys. Chem. A* **2006**, *110*, 13349−13354.
(26) Blase, X.; Attaccalite, C.; Olevano, V. *Phys. Rev. B* **2011**, *83*, 115103.
(27) Duchemin, I.; Deutsch, T.; Blase, X. *Phys. Rev. Lett.* **2012**, *109*, 167801.
(28) Hogan, C.; Palummo, M.; Gierschner, J.; Rubio, A. *J. Chem. Phys.* **2013**, *138*, 024312.
(29) Onida, G.; Reining, L.; Rubio, A. *Rev. Mod. Phys.* **2002**, *74*, 601−659.
(30) Samsonidze, G.; Jain, M.; Deslippe, J.; Cohen, M. L.; Louie, S. G. *Phys. Rev. Lett.* **2011**, *107*, 186404.
(31) Tozer, D. J. *J. Chem. Phys.* **2003**, *119*, 12697−12699.
(32) Yanai, T.; Tew, D. P.; Handy, N. C. *Chem. Phys. Lett.* **2004**, *393*, 51−57.
(33) Jain, M.; Chelikowsky, J. R.; Louie, S. G. *Phys. Rev. Lett.* **2011**, *107*, 216806.
(34) Savoie, B. M.; Jackson, N. E.; Marks, T. J.; Ratner, M. A. *Phys. Chem. Chem. Phys.* **2013**, *15*, 4538−4547.
(35) Yang, S.; Olishevski, P.; Kertesz, M. *Synth. Met.* **2004**, *141*, 171−177.
(36) Mori-Sánchez, P.; Cohen, A. J.; Yang, W. *Phys. Rev. Lett.* **2008**, *100*, 146401(1)−146401(4).
(37) Salzner, U. *J. Chem. Theory Comput.* **2007**, *3*, 1143−1157.
(38) Sutton, C.; Sears, J. S.; Coropceanu, V.; Brédas, J.-L. *J. Phys. Chem. Lett.* **2013**, *4*, 919−924.
(39) Savin, A. On degeneracy, near-degenaracy and density functional theory. In *Recent Developments and Applications of Modern Density Functional Theory*; Seminario, J. M., Ed.; Elsevier: Amsterdam, 1996; Vol. *4*, pp 327−357.
(40) Iikura, H.; Tsuneda, T.; Yanai, T.; Hirao, K. *J. Chem. Phys.* **2001**, *115*, 3540−3544.
(41) Baer, R.; Neuhauser, D. *Phys. Rev. Lett.* **2005**, *94*, 043002−4.
(42) Vydrov, O. A.; Scuseria, G. E. *J. Chem. Phys.* **2006**, *125*, 234109−9.
(43) Tsuneda, T.; Hirao, K. *WIREs Comput. Mol. Sci.* **2013**, DOI: 10.1002/wcms.1178.
(44) Chai, J.; Head-Gordon, M. *J. Chem. Phys.* **2008**, *128*, 084106−15.
(45) Seidl, A.; Görling, A.; Vogl, P.; Majewski, J. A.; Levy, M. *Phys. Rev. B* **1996**, *53*, 3764−3774.
(46) Kronik, L.; Stein, T.; Refaely-Abramson, S.; Baer, R. *J. Chem. Theory Comput.* **2012**, *8*, 1515−1531.

(47) Salzner, U.; Aydin, A. *J. Chem. Theory Comput.* **2011**, *7*, 2568−2583.
(48) Sun, H.; Autschbach, J. *ChemPhysChem* **2013**, *14*, 2450−2461.
(49) Kamiya, M.; Sekino, H.; Tsuneda, T.; Hirao, K. *J. Chem. Phys.* **2005**, *122*, 234111−10.
(50) Jacquemin, D.; Perpete, E. A.; Medved', M.; Scalmani, G.; Frisch, M. J.; Kobayashi, R.; Adamo, C. *J. Chem. Phys.* **2007**, *126*, 191108.
(51) Baer, R.; Neuhauser, D. *Phys. Rev. Lett.* **2005**, *94*, 043002−7.
(52) Livshits, E.; Baer, R. *Phys. Chem. Chem. Phys.* **2007**, *9*, 2932−2941.
(53) Baer, R.; Livshits, E.; Salzner, U. *Annu. Rev. Phys. Chem.* **2010**, *61*, 85−109.
(54) Stein, T.; Eisenberg, H.; Kronik, L.; Baer, R. *Phys. Rev. Lett.* **2010**, *105*, 266802−4.
(55) Srebro, M.; Autschbach, J. *J. Chem. Theory Comput.* **2012**, *8*, 245−256.
(56) Moore, B. I.; Srebro, M.; Autschbach, J. *J. Chem. Theory Comput.* **2012**, *8*, 4336−4346.
(57) Moore, B. I.; Autschbach, J. *ChemistryOpen* **2012**, *1*, 184−194.
(58) Pritchard, B.; Autschbach, J. *Inorg. Chem.* **2012**, *51*, 8340−8351.
(59) Cohen, A. J.; Mori-Sánchez, P.; Yang, W. *Science* **2008**, *321*, 792−794.
(60) Foster, M. E.; Wong, B. M. *J. Chem. Theory Comput.* **2012**, *8*, 2682−2687.
(61) Pandey, L.; Doiron, C.; Sears, J. S.; Brédas, J.-L. *Phys. Chem. Chem. Phys.* **2012**, *14*, 14243−14248.
(62) Körzdörfer, T.; Sears, J. S.; Sutton, C.; Brédas, J.-L. *J. Chem. Phys.* **2011**, *135*, 204107−6.
(63) Wykes, M.; Milián-Medina, B.; Gierschner, J. *Front. Chem.* **2013**, *1*, 35.
(64) Srebro, M.; Autschbach, J. *J. Phys. Chem. Lett.* **2012**, *3*, 576−581.
(65) Refaely-Abramson, S.; Sharifzadeh, S.; Govind, N.; Autschbach, J.; Neaton, J. B.; Baer, R.; Kronik, L. *Phys. Rev. Lett.* **2012**, *109*, 226405−5.
(66) Casida, M. E. Time-dependent density functional response theory for molecules. In *Recent advances in density functional methods*, Chong, D. P., Ed.; World Scientific: Singapore, 1995; Vol. *1*, pp 155−192.
(67) Grüning, M.; Gonze, X. *Phys. Rev. B* **2007**, *76*, 035126.
(68) Brothers, E. N.; Izmaylov, A. F.; Normand, J. O.; Barone, V.; Scuseria, G. E. *J. Chem. Phys.* **2008**, *129*, 011102.
(69) Heyd, J.; Scuseria, G. E.; Ernzerhof, M. *J. Chem. Phys.* **2003**, *118*, 8207−8215.
(70) Heyd, J.; Peralta, J. E.; Scuseria, G. E.; Martin, R. L. *J. Chem. Phys.* **2005**, *123*, 174101.
(71) Schuchardt, K. L.; Didier, B. T.; Elsethagen, T.; Sun, L.; Gurumoorthi, V.; Chase, J.; Li, J.; Windus, T. L. *J. Chem. Inf. Model.* **2007**, *47*, 1045−1052.
(72) Frisch, M. J.; Trucks, G. W.; Schlegel, H. B.; Scuseria, G. E.; Robb, M. A.; Cheeseman, J. R.; Scalmani, G.; Barone, V.; Mennucci, B.; Petersson, G. A.; Nakatsuji, H.; Caricato, M.; Li, X.; Hratchian, H. P.; Izmaylov, A. F.; Bloino, J.; Zheng, G.; Sonnenberg, J. L.; Hada, M.; Ehara, M.; Toyota, K.; Fukuda, R.; Hasegawa, J.; Ishida, M.; Nakajima, T.; Honda, Y.; Kitao, O.; Nakai, H.; Vreven, T.; Montgomery, J. A., Jr.; Peralta, J. E.; Ogliaro, F.; Bearpark, M.; Heyd, J. J.; Brothers, E.; Kudin, K. N.; Staroverov, V. N.; Kobayashi, R.; Normand, J.; Raghavachari, K.; Rendell, A.; Burant, J. C.; Iyengar, S. S.; Tomasi, J.; Cossi, M.; Rega, N.; Millam, J. M.; Klene, M.; Knox, J. E.; Cross, J. B.; Bakken, V.; Adamo, C.; Jaramillo, J.; Gomperts, R.; Stratmann, R. E.; Yazyev, O.; Austin, A. J.; Cammi, R.; Pomelli, C.; Ochterski, J. W.; Martin, R. L.; Morokuma, K.; Zakrzewski, V. G.; Voth, G. A.; Salvador, P.; Dannenberg, J. J.; Dapprich, S.; Daniels, A. D.; Farkas, O.; Foresman, J. B.; Ortiz, J. V.; Cioslowski, J.; ; Fox, D. J. *Gaussian 09*, Revision A.02; Gaussian, Inc.: Wallingford CT, 2009.
(73) Becke, A. D. *J. Chem. Phys.* **1993**, *90*, 5648−5652.
(74) Lee, C.; Yang, W.; Parr, R. G. *Phys. Rev. B* **1988**, *37*, 785−789.
(75) Bylaska, E. J.; de Jong, W. A.; Govind, N.; Kowalski, K.; Straatsma, T. P.; Valiev, M.; van Dam, J. J.; Wang, D.; Apra, E.; Windus, T. L.; Hammond, J.; Autschbach, J.; Aquino, F.; Nichols, P.; Hirata, S.; Hackler, M. T.; Zhao, Y.; Fan, P.-D.; Harrison, R. J.; Dupuis, M.; Smith, D. M. A.; Glaesemann, K.; Nieplocha, J.; Tipparaju, V.; Krishnan, M.; Vazquez-Mayagoitia, A.; Jensen, L.; Swart, M.; Wu, Q.; Van Voorhis, T.; Auer, A. A.; Nooijen, M.; Crosby, L. D.; Brown, E.; Cisneros, G.; Fann, G. I.; Fruchtl, H.; Garza, J.; Hirao, K.; Kendall, R.; Nichols, J. A.; Tsemekhman, K.; Wolinski, K.; Anchell, J.; Bernholdt, D.; Borowski, P.; Clark, T.; Clerc, D.; Dachsel, H.; Deegan, M.; Dyall, K.; Elwood, D.; Glendening, E.; Gutowski, M.; Hess, A.; Jaffe, J.; Johnson, B.; Ju, J.; Kobayashi, R.; Kutteh, R.; Lin, Z.; Littlefield, R.; Long, X.; Meng, B.; Nakajima, T.; Niu, S.; Pollack, L.; Rosing, M.; Sandrone, G.; Stave, M.; Taylor, H.; Thomas, G.; van Lenthe, J.; Wong, A.; Zhang, Z. *NWChem, A Computational Chemistry Package for Parallel Computers*, version 6 (2013 developer's version); Pacific Northwest National Laboratory: Richland, Washington, 2013.
(76) Baerends, E. J.; Ziegler, T.; Autschbach, J.; Bashford, D.; Bérces, A.; Bickelhaupt, F. M.; Bo, C.; Boerrigter, P. M.; Cavallo, L.; Chong, D. P.; Deng, L.; Dickson, R. M.; Ellis, D. E.; van Faassen, M.; Fan, L.; Fischer, T. H.; Fonseca Guerra, C.; Ghysels, A.; Giammona, A.; van Gisbergen, S. J. A.; Götz, A. W.; Groeneveld, J. A.; Gritsenko, O. V.; Grüning, M.; Gusarov, S.; Harris, F. E.; van den Hoek, P.; Jacob, C. R.; Jacobsen, H.; Jensen, L.; Kaminski, J. W.; van Kessel, G.; Kootstra, F.; Kovalenko, A.; Krykunov, M. V.; van Lenthe, E.; McCormack, D. A.; Michalak, A.; Mitoraj, M.; Neugebauer, J.; Nicu, V. P.; Noodleman, L.; Osinga, V. P.; Patchkovskii, S.; Philipsen, P. H. T.; Post, D.; Pye, C. C.; Ravenek, W.; Rodríguez, J. I.; Ros, P.; Schipper, P. R. T.; Schreckenbach, G.; Seldenthuis, J. S.; Seth, M.; Snijders, J. G.; Solà, M.; Swart, M.; Swerhone, D.; te Velde, G.; Vernooijs, P.; Versluis, L.; Visscher, L.; Visser, O.; Wang, F.; Wesolowski, T. A.; van Wezenbeek, E. M.; Wiesenekker, G.; Wolff, S. K.; Woo, T. K.; Yakovlev, A. L. *Amsterdam Density Functional, SCM, Theoretical Chemistry*; Vrije Universiteit, Amsterdam: The Netherlands, 2006; http://www.scm.com.
(77) Siegert, S.; Vogeler, F.; Marian, C. M.; Weinkauf, R. *Phys. Chem. Chem. Phys.* **2011**, *13*, 10350−10363.
(78) da Silva Filho, D. A.; Coropceanu, V.; Fichou, D.; Gruhn, N. E.; Bill, T. G.; Gierschner, J.; Cornil, J.; Brédas, J.-L. *Phil. Trans. R. Soc. A* **2007**, *365*, 1435−1452.
(79) Seixas de Melo, J.; Elisei, F.; Gartner, C.; Aloisi, G. G.; Becker, R. S. *J. Phys. Chem. A* **2000**, *104*, 6907−6911.
(80) Alemán, C.; Torras, J.; Casanovas, J. *Chem. Phys. Lett.* **2011**, *511*, 283−287.
(81) Jones, D.; Guerra, M.; Favaretto, L.; Modelli, A.; Fabrizio, M.; Distefano, G. *J. Phys. Chem.* **1990**, *94*, 5761−5766.
(82) Perdew, J. P.; Burke, K.; Ernzerhof, M. *Phys. Rev. Lett.* **1996**, *77*, 3865−3868.
(83) Adamo, C.; Barone, V. *J. Chem. Phys.* **1999**, *110*, 6158−6170.
(84) Levy, M.; Perdew, J. P.; Sahni, V. *Phys. Rev. A* **1984**, *30*, 2745−2748.
(85) Gritsenko, O.; Baerends, E. J. *J. Chem. Phys.* **2004**, *121*, 655−660.
(86) Yang, W.; Cohen, A. J.; Mori-Sanchez, P. *J. Chem. Phys.* **2012**, *136*, 204111−13.
(87) Stein, T.; Kronik, L.; Baer, R. *J. Chem. Phys.* **2009**, *131*, 244119−5.
(88) Kuritz, N.; Stein, T.; Baer, R.; Kronik, L. *J. Chem. Theory Comput.* **2011**, *7*, 2408−2415.
(89) Stein, T.; Autschbach, J.; Govind, N.; Kronik, L.; Baer, R. *J. Phys. Chem. Lett.* **2012**, *3*, 3740−3744.
(90) Perdew, J. P.; Parr, R. G.; Levy, M.; Balduz, J. L., Jr. *Phys. Rev. Lett.* **1982**, *49*, 1691−1694.
(91) Dunning, T. H. *J. Chem. Phys.* **1989**, *90*, 1007−1023.
(92) Schafer, A.; Huber, C.; Ahlrichs, R. *J. Chem. Phys.* **1994**, *100*, 5829−5835.
(93) Chung, T.; Kaufman, J. H.; Heeger, A. J.; Wudl, F. *Phys. Rev. B* **1984**, *30*, 702.
(94) Kobayashi, M.; Chen, J.; Chung, T. C.; Moraes, F.; Heeger, A. J.; Wudl, F. *Synth. Met.* **1984**, *9*, 77−86.

(95) Meier, H.; Stalmach, U.; Kolshorn, H. *Acta Polym.* **1997**, *48*, 379−384.
(96) Nakanishi, H.; Sumi, N.; Aso, Y.; Otsubo, T. *J. Org. Chem.* **1998**, *63*, 8632−8633.
(97) Aryasetiawan, F.; Gunnarsson, O. *Rep. Prog. Phys.* **1998**, *61*, 237−312.
(98) vanSchilfgaarde, M.; Kotani, T.; Faleev, S. *Phys. Rev. Lett.* **2006**, *96*, 226402.
(99) Bäuerle, P. Sulfur-Containing Oligomers. In *Electronic Materials: The Oligomer Approach*; Müllen, K., Egner, G., Eds.; Wiley-VCH Verlag GmbH: Weinheim, 1998; pp 105−197.
(100) Lap, D. V.; Grebner, D.; Rentsch, S. *J. Phys. Chem. A* **1997**, *101*, 107−112.
(101) Kraak, A.; Wynberg, H. *Tetrahedron* **1968**, *24*, 3881−3885.
(102) Salzner, U.; Karalti, O.; Durdağı, S. *J. Mol. Model.* **2006**, *12*, 687−701.
(103) Janesko, B. G. *J. Chem. Phys.* **2011**, *134*, 184105.
(104) Wong, B. M.; Cordaro, J. G. *J. Phys. Chem. C* **2011**, *115*, 18333−18341.
(105) Dietrich, M.; Heinze, J.; Heywang, G.; Jonas, F. *J. Electroanal. Chem.* **1994**, *369*, 87−92.
(106) Glenis, S.; Benz, M.; LeGoff, E.; Schindler, J. L.; Kannewurf, C. R.; Kanatzidis, M. G. *J. Am. Chem. Soc.* **1993**, *115*, 12519−12525.
(107) Hiberty, P. C.; Shaik, S. *Phys. Chem. Chem. Phys.* **2004**, *6*, 224−231.
(108) Moore, B. I.; Autschbach, J. *J. Chem. Theory Comput.* **2013**, *9*, 4991−5003.
(109) Körzdörfer, T.; Parrish, R. M.; Sears, J. S.; Sherrill, C. D.; Brédas, J.-L. *J. Chem. Phys.* **2012**, *137*, 124305.
(110) Cohen, A. J.; Mori-Sánchez, P.; Yang, W. *Chem. Rev.* **2012**, *112*, 289−320.
(111) Mulliken, R. S. *J. Am. Chem. Soc.* **1950**, *72*, 600−608.
(112) Stein, T.; Kronik, L.; Baer, R. *J. Am. Chem. Soc.* **2009**, *131*, 2818−2820.
(113) Autschbach, J. *ChemPhysChem* **2009**, *10*, 1757−1760.
(114) Neugebauer, J.; Gritsenko, O.; Baerends, E. J. *J. Chem. Phys.* **2006**, *124*, 214102−11.
(115) Peach, M. J. G.; Benfield, P.; Helgaker, T.; Tozer, D. J. *J. Chem. Phys.* **2008**, *128*, 044118−8.
(116) Guido, C. A.; Cortona, P.; Mennucci, B.; Adamo, C. *J. Chem. Theory Comput.* **2013**, *9*, 3118−3126.